Atmósfera 24(4), 435-446 (2011)

Net radiation estimation under pasture and forest in Rondônia, Brazil, with TM Landsat 5 images

C. A. COSTA DOS SANTOS, R. L. DO NASCIMENTO, T. V. R. RAO
Unidade Acadêmica de Ciências Atmosféricas, Universidade Federal de Campina Grande, Avenida Aprígio Veloso, 882, Bodocongó, Campina Grande, PB, CEP: 58109-970, Brasil
Corresponding author; C. A. Costa dos Santos e-mails: carlostorm@gmail.com; carlos@dca.ufc.edu.br

A. O. MANZI
Programa de Grande Escala da Biosfera-Atmosfera na Amazônia, Instituto Nacional de Pesquisas da Amazônia, Avenida André Araújo, 2936, Aleixo, CEP 69060-001 Manaus, AM, Brasil

Received March 29, 2010; accepted June 14, 2011

RESUMEN

El objetivo principal de este estudio es obtener la distribución espacial de la radiación neta (R_N) en dos cubiertas vegetales contrastantes (bosque y pasto) mediante el algoritmo SEBAL, y analizar su funcionamiento cuando es aplicado en condiciones atmosféricas húmedas tropicales. Este estudio se realizó en el estado de Rondônia, en el noroeste de Brasil, utilizándose cuatro imágenes Landsat TM, así como datos de un modelo digital del terreno. Los principales resultados indican cómo los coeficientes de correlación entre los valores estimados (SEBAL) y medidos de R_N, y el albedo son de 0.97 y 0.88, respectivamente. Estos resultados muestran como SEBAL constituye una importante herramienta para su aplicación en estudios hidrológicos y ambientales, y para obtener variaciones espaciales y temporales coherentes de las características de la superficie, apoyando la mejora y validación de las parametrizaciones del modelo. Sin embargo, las aplicaciones de las técnicas de teledetección en climas húmedos tropicales son difíciles, debido a la constante presencia de nubes como consecuencia de procesos convectivos.

ABSTRACT

The main objective of this study is to obtain the spatial distribution of net radiation (R_N) in two contrasting vegetation covers (forest and pasture) through the SEBAL algorithm, and to analyze its performance when applied to tropical humid atmospheric conditions. This study was conducted in the state of Rondônia in northwestern Brazil, using four Landsat TM images, as well as, digital elevation model data. The correlation coefficients between estimated (SEBAL) and measured values of R_N, and surface albedo are of 0.97 and 0.88, respectively. These results present SEBAL as an important tool to be used in hydrological and environmental studies, and to obtain coherent temporal and spatial variations of surface characteristics, helping in the improvement and validation of model parameterizations. However, the applications of remote sensing techniques in tropical humid climates are difficult, because of the existence of a constant presence of convective clouds.

Keywords: Humid climate, Amazonian rainforest, evapotranspiration, spatial variability.

1. Introduction

Studies have shown that the Amazonian forests have a large influence on regional and global climates (Malhi *et al.*, 2008). Thus, the conversion of forest to pasture and/or agricultural lands may cause large impacts on the regional hydrological, ecological and climatological processes (von Randow *et al.*, 2004). The Large Scale Biosphere-Atmosphere Experiment in Amazonia (LBA) is an international research initiative led by Brazil. It is designed to create the new knowledge needed to understand the climatological, ecological, biogeochemical, and hydrological functioning of Amazonia, the impact of land use change on these functions, and the interactions between Amazonia and the earth system.

Net radiation (R_N) is the most important parameter for computing the evapotranspiration, and is a driving force for other physical and biological processes (Samani *et al.*, 2007). It is defined as the difference between the incoming and outgoing radiation fluxes (longwave and shortwave) at the Earth's surface, and is used for different applications, such as climate monitoring, weather forecast and agricultural meteorology (Bisht *et al.*, 2005). Net radiation data are rarely available, and does not represent the spatial variability. Remote sensing is an innovative tool to observe land surface processes on a large spatial scale and low cost-effective (Cai and Sharma, 2010), hence several studies have tried to estimate R_N through the combination of remote sensing observations with atmospheric and surface data (Bastiaanssen *et al.*, 1998; Roerink *et al.*, 2000; Bisht *et al.*, 2005; Rimóczi-Paál, 2005; Silva *et al.*, 2005; Samani *et al.*, 2007; Di Pace *et al.*, 2008; Ryu *et al.,* 2008; Wang and Liang, 2009).

The main objective of this study is to obtain the spatial distribution of R_N in two contrasting vegetation covers, tall tropical rainforest and short grassland, by using remote sensing techniques, and to analyze the performance of the SEBAL algorithm when applied to tropical humid conditions. The reason for this study is the deficiency of spatial R_N information and the fact of this algorithm has been vastly used in arid and semi-arid regions.

2. Materials and methods

This study was conducted in the state of Rondônia in northwestern Brazil during the year of 2008. The forest site is called Biological Reserve of Rio Jaru (Rebio-Jaru) located at 10º4'48.00"S; 61º55'48.00"W and 120 m above the sea level. The grassland or pasture site is located in the cattle ranch called Fazenda Nossa Senhora (FNS) presenting geographical coordinates of 10º45'0.00"S; 62º22'12.00"W and 293 m above sea level. The geographical location of the study area, in Rondônia, for two different land covers (pasture and forest) is illustrated in Figure 1. The list of meteorological variables measured, instruments and measurement heights are shown in Table I.

Four Landsat thematic mapper (TM) images (day of the year (DOY) = 187, 203, 219 and 267) were acquired around 10:00 a.m. local time in 2008. The spatial resolution for the reflectance bands of TM is 30 x 30 m and 120 x 120 m for the thermal band. It was necessary to resample the thermal band to the same size of the reflectance bands, as well as, the digital elevation model (DEM) data which has 90 m resolution.

The Landsat Program is a series of Earth-observing satellite missions jointly managed by NASA and the US Geological Survey. Since 1972, Landsat satellites have collected information about

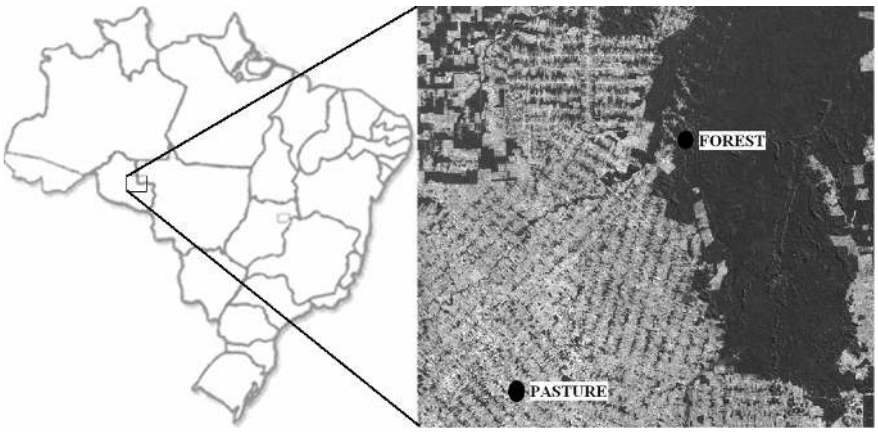

Fig. 1. Geographical location of the study area, in Rondônia State, Brazil. Different land cover (pasture and forest) are shown in gray and dark black, respectively.

Table I. List of meteorological variables measurements, instruments and measurement heights in pasture and forest land covers in Rondônia, Brazil.

Meteorological variable measurements	Instruments	Height (m) FNS (pasture)	Height (m) Rebio Jaru (forest)
Incident and reflected shortwave radiation	Pyranometer Kipp & Zonen (CM21)	6.5	19.3
Incident and emitted longwave radiation	Pyrgeometer Kipp & Zonen (CG1)	6.5	19.3
Air temperature	Vaisala thermohygrometer HMP35A	8.3	60.0
Wind speed	Cup anemometer Vector A100R	9.3	61.1
Surface radiative temperature	Infrared sensor Heimann (KT15)	8.0	59.1
Rainfall	Rain gauge EM ARG-100	0.5	60.3

Earth from space. This science, known as remote sensing, has matured with the Landsat Program. Landsat satellites have taken specialized digital photographs of Earth's continents and surrounding coastal regions for over three decades, enabling people to study many aspects of our planet and to evaluate the dynamic changes caused by both natural processes and human practices. The Thematic mapper (TM) sensor is an advanced, multispectral scanner; the data are sensed in seven spectral bands simultaneously, as shown in Table II.

Algorithm for R_N estimation

Surface Energy Balance Algorithm for Land (SEBAL) (Bastiaanssen *et al.*, 1998) uses spectral radiances recorded by satellite sensors and meteorological measurements to solve the energy balance (*net radiation = soil heat flux + sensible heat flux + latent heat flux*) at the land surface (Gao *et al.*, 2008). To obtain surface energy fluxes from any land surface requires mainly energy

Table II. Detailed descriptions of the TM Landsat 5 spectral bands.

Band number	Spectral range (μm)	Resolution (m)
1	0.45-0.52	30
2	0.52-0.60	30
3	0.63-0.69	30
4	0.76-0.90	30
5	1.55-1.75	30
6	10.4-12.5	120
7	2.08-2.35	30

inputs, i.e. shortwave and longwave radiation, and remote sensing can provide these inputs at a reasonable spatial and temporal scale. In this study, R_N (energy input) was estimated using the relationship proposed by Bastiaanssen *et al.* (1998):

$$R_N = R_S\downarrow (1 - \alpha) + R_L\downarrow - R_L\uparrow - R_L\downarrow (1 - \varepsilon) \quad (1)$$

where $R_S\downarrow$ (W m^{-2}) is the incoming direct and diffuse shortwave radiation at surface; α (dimensionless) is the surface albedo, i.e. the ratio of reflected radiation to the incident shortwave radiation; $R_L\downarrow$ (W m^{-2}) is the incoming longwave radiation from the atmosphere; $R_L\uparrow$ (W m^{-2}) is the outgoing longwave radiation emitted from the surface to the atmosphere; and ε (dimensionless) is the surface emissivity, which is the ratio of the radiant emittance from a grey body to the emittance of a blackbody (Melesse *et al.*, 2008).

$R_S\downarrow$ is a function of several factors, such as: solar elevation, solar radiation intensity, atmospheric transmittance and topographic correction. In this study, $R_S\downarrow$ was estimated as:

$$R_S\downarrow = \frac{I_0 \tau_{SW}}{d^2 \sin\theta} \quad (2)$$

where I_0 is the solar constant (1367 W m^{-2}); θ is the solar inclination angle (radians); d (astronomical units) is the relative distance between the Earth and the Sun; and τ_{SW} is the one way atmospheric transmissivity, computed using the procedures adapted by Allen *et al.* (1998):

$$\tau_{SW} = 0.75 + 2\text{x}10^{-5} Z \quad (3)$$

where Z (m) is the elevation, obtained from the DEM.

In SEBAL algorithm, the surface albedo is computed by correcting the albedo at the top of the atmosphere (α_{toa}) for atmospheric transmissivity:

$$\alpha = \frac{\alpha_{toa} - \alpha_{path\_radiance}}{\tau_{SW}^2} \quad (4)$$

where $\alpha_{path\_radiance}$ is the average portion of the incoming solar radiation across all bands that is back-scattered to the satellite before it reaches the surface of Earth, which varies between 0.025 and 0.04. Bastiaanssen *et al.* (1998) recommends the use of $\alpha_{path\_radiance} = 0.03$.

$R_L\downarrow$ was estimated using the following equation:

$$R_L\downarrow = \sigma \varepsilon_a T_a^4 \tag{5}$$

where σ is the Stefan-Boltzmann constant ($\sigma = 5.67 \times 10^{-8}$ $Wm^{-2}K^{-4}$); T_a is the near surface air temperature (K); and ε_a is the atmospheric emissivity (dimensionless) obtained through an empirical equation proposed by Bastiaanssen *et al.* (1998):

$$\varepsilon_a = -0.85(1n\ \tau_{SW})^{0.09} \tag{6}$$

The longwave radiation emitted from the surface of Earth to the atmosphere ($R_L\uparrow$) was determined by the Stefan-Boltzmann law:

$$R_L\uparrow = \sigma \varepsilon T_S^4 \tag{7}$$

where ε is the surface emissivity and T_S is the surface temperature (K). In SEBAL, the surface emissivity is estimated using the normalized difference vegetation index (NDVI) and an empirically derived scheme (Bastiaanssen *et al.*, 1998):

$$\varepsilon = 1.009 + 0.047(1n\ NDVI) \tag{8}$$

if NDVI > 0 and ε = 1 for NDVI < 0 (e.g. for water).

Surface temperature (T_S) was obtained from the thermal band (spectral range from 10.4 to 12.5 mm) (band 6 of the Landsat 5 - TM sensor) radiance values using the simplified Plank's equation and corrected using ε:

$$T_S = \frac{k_2}{1n(\frac{\varepsilon k_1}{R} + 1)} \tag{9}$$

where $k_1 = 607.76$ W m^{-2} sr^{-1} μm^{-1} and $k_2 = 1260.56$ K are calibration constants, and R is a linear function of the digital number (DN) equal to:

$$R = a \times DN + b \tag{10}$$

where $a = 0.055158$ W m^{-2} sr^{-1} μm^{-1} and $b = 1.2378$ W m^{-2} sr^{-1} μm^{-1} (Melesse *et al.*, 2008).

3. Results and discussions

Tables III and IV present the comparisons of the temporal distribution of estimated net radiation (R_N) and surface albedo (α), using the SEBAL algorithm, with measured values at the FNS (pasture) and Rebio Jaru (forest) sites, respectively. The temporal distribution of NDVI for the different sites is also shown. In Table III, the R_N maximum mean percentage error (MPE) of 16% is shown for the DOY 267 and the minimum MPE of 7% for DOY 219. Similar results are shown for α values, with maximum and minimum MPE of 39 and 0% for the DOY 267 and 219, respectively. The NDVI values decreased from 0.48 to 0.12. This decrease occurs due to the intensification of the dry season affecting the grass development (pasture); however, the minimum value of 0.12 is related to the burning activities in the area, which reduce drastically the NDVI values. Thus, the pastures site presented lower NDVI values due to the water deficit while the forest site presented higher NDVI values because these regions have more soil water content and green biomass.

Table III. Comparison of the estimated net radiation (R_N) and surface albedo (α), obtained by remote sensing algorithm, with measured values at the FNS site, as well as, the temporal distribution of the normalized difference vegetation index (NDVI) and the Mean Percentage Error (MPE).

DOY	R_N (SEBAL) (Wm^{-2})	R_N (Measured) (Wm^{-2})	MPE (%)	α (SEBAL)	α (Measured)	MPE (%)	NDVI (SEBAL)
187	500	450	11	0.18	0.21	–14	0.48
203	492	450	9	0.19	0.21	–10	0.39
219	497	465	7	0.22	0.22	0	0.31
267	663	573	16	0.11	0.18	–39	0.12

It can be observed that the albedo in pasture is larger than in forest. This difference between them is due to the variation in vegetation coloration; in other words, the forest area being darker reflects less energy than the pasture. Besides the coloration of the vegetation, the vertical structure of the forest (more than 30 meters of height on average), propitiates the absorption of solar rays that penetrate the forest canopy and are absorbed in the inferior layers.

In Table IV, the R_N maximum MPE of 12% is shown for the DOY 203 and the minimum MPE of 4% for the DOY 267. Similar results are shown for α values, with maximum and minimum MPE of 17% and 0% for the DOY 203 and 267, respectively. The NDVI values stayed almost constant during the study period, showing that the forest has a different behavior compared to

Table IV. Comparison of the estimated R_N and α, obtained by remote sensing algorithm, with measured values at the Rebio Jaru site, as well as, the temporal distribution of NDVI and the MPE.

DOY	R_N (SEBAL) (Wm^{-2})	R_N (Measured) (Wm^{-2})	MPE (%)	α (SEBAL)	α (Measured)	MPE (%)	NDVI (SEBAL)
187	574	548	5	0.10	0.12	–17	0.65
203	592	529	12	0.10	0.12	–17	0.72
219	607	550	10	0.12	0.13	–8	0.65
267	734	703	4	0.12	0.12	0	0.69

pasture during the dry season. In both the sites, the R_N estimated and measured values presented a significant increase for the DOY 267, showing the high solar energy supply in this region under clear-sky conditions during the dry season, which is used as driving force for different physical processes, such as surface heating, plant transpiration and water evaporation. All these processes are important for the environment, and the conversion of forest to pasture change drastically the net radiation at land surface, inducing changes in the regional climate.

The comparison between Tables III and IV shows that R_N values are higher in forested areas because they have lower α, i.e. reflect less solar (shortwave) radiation, when compared to deforested areas (pasture, for example). The surface albedo is the main factor that affects the land surface radiation balance and has frequently been considered in studies of regional and global climate. Oguntoyinbo (1970) found an average α of 12% for forested areas and for non-forested areas α varied from 15 to 21%. Shuttleworth *et al.* (1984) identified an average α of 12.3 ± 0.2% for a tropical rainforest near Manaus, Brazil. Culf *et al.* (1996) found an average α of 13.4 and 18% for Amazonian forest and three pasture sites, respectively. All these results corroborate those showed in this study.

The applications of remote sensing techniques in tropical humid climates are difficult. The main problem is the constant presence of clouds due to the convective process which is an important mechanism in heating the tropical atmosphere. To illustrate this difficulty, the diurnal behavior of the four radiation components, incoming and outgoing shortwave (RS_in and RS_out), and longwave (RL_in and RL_out) radiations, for the pasture and forest sites, respectively are shown in Figures 2 and 3. In fact, clouds were present on all the days of study at noon or afternoon for the FNS and Rebio Jaru sites, except for the DOY 187 at the Rebio Jaru station, which was a clear-sky day. It was possible to apply remote sensing techniques and SEBAL algorithm to obtain the instantaneous R_N because the Landsat satellite has a morning overpass over the study area (about 10:00 a.m. local time), and during this time no cloud interferences were found.

It is interesting to note that the largest variability of the incoming solar radiation occurred on the pasture than on the forest, especially in the afternoon. This behavior is caused by the temperature gradient between the two ground covers, that generate drainage of air of the forest (more cold and denser) to the pasture (hotter and less dense) and movement of ascending air on the pasture, that transports upward the water vapor, which condenses and forms clouds over the pasture.

The observed behavior of the incoming longwave radiation (RL_in) shows that its values in the pasture, in general, were larger than in the forest, due to higher temperature of the air in the pasture than in the forest during the day. At night, although the temperature of the air at the surface is lesser in the pasture than in the forest, the average temperature of the lower troposphere is larger above the pasture (Galvão and Fisch, 2000). It has been observed larger values of outgoing longwave radiation in the pasture and smaller values in the forest during the day, and the inverse behavior is observed during the night. Those behaviors at night or during the day are due to the surface temperature. During the night the pasture surface tends to lose heat faster to the atmosphere becoming colder than the forest surface.

Figures 4a and 4b show the correlations between the estimated values of R_N and α by SEBAL algorithm and measured values at the study stations (pasture and forest). The high correlations of R_N estimated (SEBAL) and measured values with correlation coefficient (R) of 0.97 are presented in Figure 4a, showing the efficiency of the simple schemes of SEBAL algorithm to obtain the radiative fluxes. The correlations between estimated and measured values of α are shown in Figure 4b, which presents R value of 0.88.

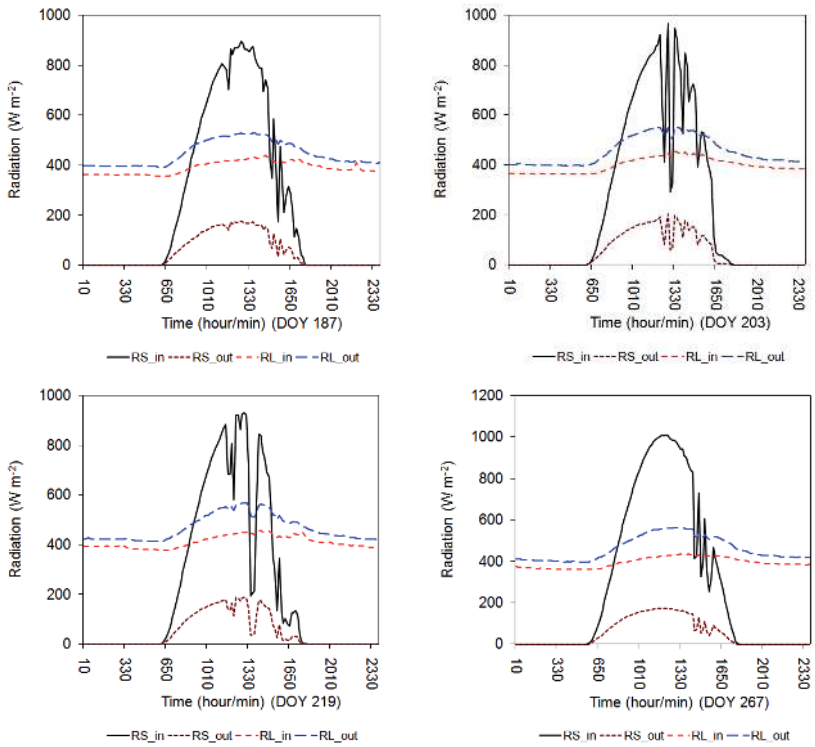

Fig. 2. Diurnal behavior of the incoming and outgoing shortwave (RS_in and RS_out) and longwave (RL_in and RL_out) radiation for different dates at the pasture site (FNS).

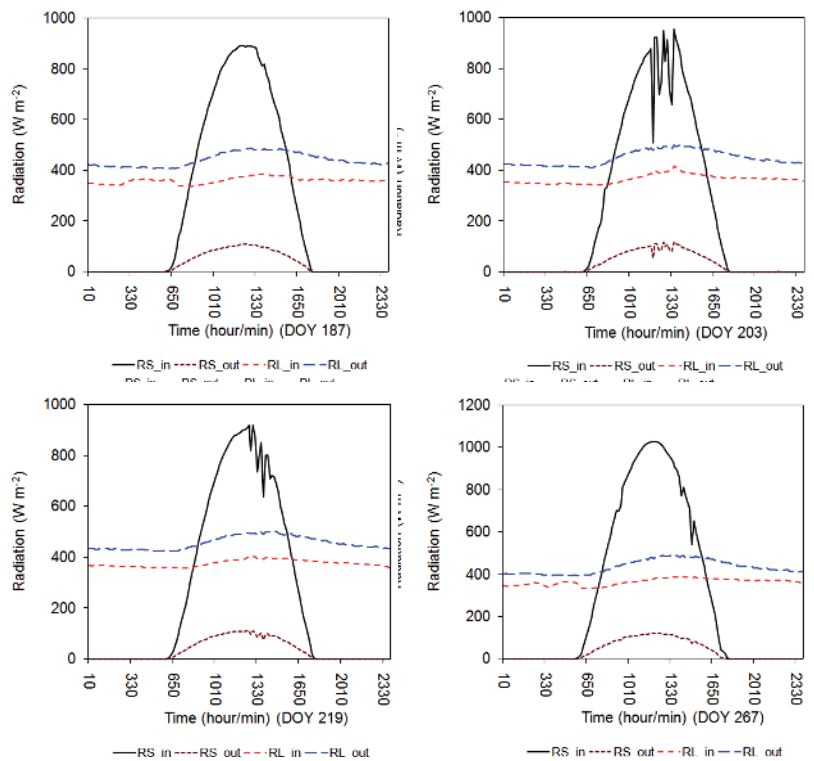

Fig. 3. Diurnal behavior of the incoming and outgoing shortwave (RS_in and RS_out) and longwave (RL_in and RL_out) radiation for different dates at the Rebio Jaru site (forest).

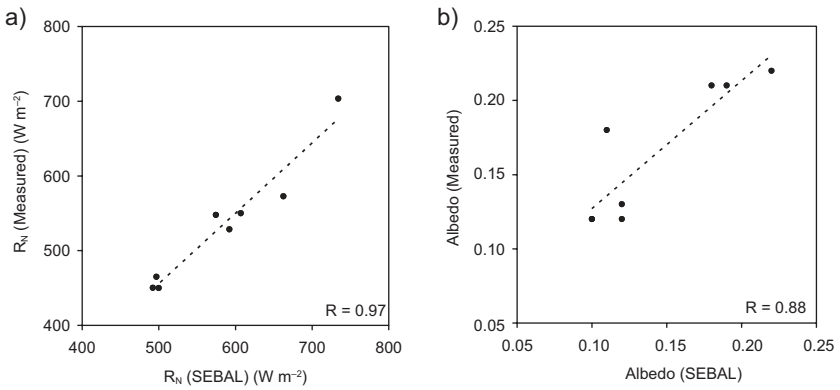

Fig. 4. Correlations between the estimated values by the SEBAL algorithm and measured values of R_N (a) and surface albedo (b) at the study area.

The spatial distribution of R_N for the DOY 187, 203, 219 and 267 are shown in Figures 5, 6, 7 and 8, respectively. The dark black areas represent lower values of R_N, while the gray areas mean higher values of R_N. In the figures, lower values of R_N are in pasture lands or bare soil, which have higher albedo, and higher values are in forest and rivers which absorb more energy to use in the different physical processes. From the figures, it is clear that the conversion of forest to pasture lands influences the environmental parameters, such as the increase of the surface albedo, and in consequence the decrease of the net radiation. These studied parameters (net radiation and surface albedo) have been evaluated with observations and satellite measurements. Measured data are fundamental to validate model results, especially because they represent more realistically a specific studied site. However, they show operational difficulties, are expensive to obtain and usually limited to a small area and do not represent the spatial variability. On the other hand, remote sensing is an important tool to obtain coherent temporal and spatial variations of surface characteristics, such as R_N and α, aiding improvement and validation of model parameterization.

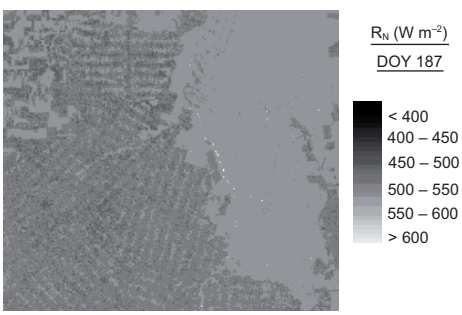

Fig. 5. Spatial distribution of R_N for different land covers (including pasture and forest), in the DOY 187 of 2008, in Rondônia, Brazil.

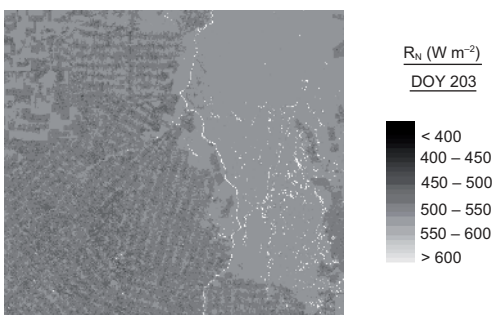

Fig. 6. Spatial distribution of R_N for different land covers (including pasture and forest), in the DOY 203 of 2008, in Rondônia, Brazil.

It is observed in this study that the R_N in forest, as well as in pasture, follows the shortwave radiation oscillations which represent the most influential component in R_N. It is possible to identify that R_N in the pasture site is less than that in forest site, because less radiation is stored in the pasture.

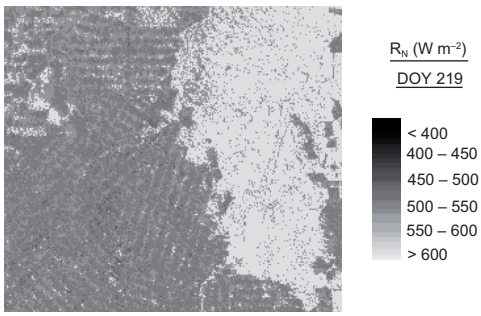

Fig. 7. Spatial distribution of R_N for different land covers (including pasture and forest), in the DOY 219 of 2008, in Rondônia, Brazil.

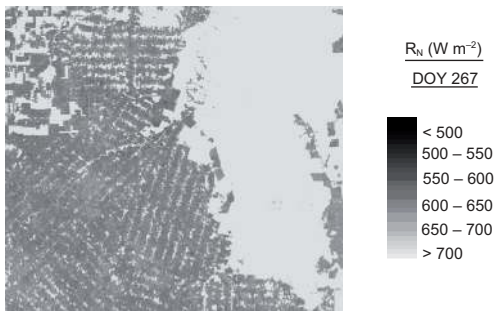

Fig. 8. Spatial distribution of R_N for different land covers (including pasture and forest), in the DOY 267 of 2008, in Rondônia, Brazil.

Smaller values of the R_N are observed in pasture area and larger values in forest area during the day. This behavior is due to the albedo, since during the day, the R_N is dominated by the radiative changes of short waves (incoming and outgoing). But there is also a contribution of the longwave net radiation, with the pasture losing more longwave radiation than the forest.

The results presented in this study are helpful in understanding the spatial variability of the radiative fluxes, as well as the net radiation, which is the fundamental quantity of energy balance at the earth's surface. The partitioning of R_N into energy balance components, especially evapotranspiration, which is a term describing the transport of water into the atmosphere from surfaces, including soil (soil evaporation), and from vegetation (transpiration), is firmly coupled with changes in land use and global climate conditions (Ryu *et al.*, 2008). For regional water resources, through the evapotranspiration models which require R_N as the core input parameter, an accurate estimation of R_N is essential. These results are also helpful in understanding the spatial behavior of the land surface temperature (LST), which is a key parameter in the physics of land surface processes because it is involved in the energy balance as well as in the evapotranspiration and change in the land surface processes (for example, the deforestation activities as presented in the study area). The extensive requirement of LST for environmental studies and management activities of the Earth's resources has made the remote sensing of LST an important academic topic during the last two decades (Peres and DaCamara, 2004), and one of the most important parameters in all surface–atmosphere interactions and energy fluxes between the ground and the atmosphere.

4. Conclusions

In this study, we employed the SEBAL algorithm to obtain the four radiation components and R_N from four Landsat 5-TM images over an interface between two distinct land covers, forest and pasture, in Rondônia, Brazil. The main results found can be summarized as follows:

1) The comparisons of the temporal distribution of R_N, using the SEBAL algorithm, with surface measured values at the FNS (pasture) site have shown maximum and minimum MPE of 16% and 7%, respectively. For the Rebio Jaru (forest) site the maximum and minimum MPE were of 12% and 4%, respectively.
2) The α estimations by SEBAL for pasture and forest have shown similarities with previous study.

3) The correlation coefficients between estimated (SEBAL) and measured values of R_N and α are of 0.97 and 0.88, respectively.
4) These results present SEBAL as an important tool to be used in hydrological and environmental studies, and to obtain coherent temporal and spatial variations of surface characteristics, helping in the improvement and validation of model parameterizations. However, the applications of remote sensing techniques in tropical humid climates are difficult, because of the existence of convective clouds.

Acknowledgements

The authors are grateful for the research fellowship provided by Conselho Nacional de Desenvolvimento Científico e Tecnológico (CNPq) to the first author and for funding the Project Nº. 556816/2009-9. This research was also supported by the Large Scale Biosphere-Atmosphere Program in Amazonia (LBA)/INPA. We thank the micrometeorology team of LBA in Ji-Paraná-RO and Manaus-AM, Brazil.

References

Allen R. G., L. S. Pereira, D. Raes and M. Smith, 1998. Crop evapotranspiration: guidelines for computing crop requirements. FAO Irrigation and Drainage Paper No. 56, Rome, Italy, 282 pp.

Bastiaanssen W. G. M., M. Menenti, R. A. Feddes and A. A. Holtslag, 1998. A remote sensing surface energy balance algorithm for land (SEBAL). 1. Formulation. *J. Hydrol.* **212-213**, 198-212.

Bisht G., V. Venturini, S. Islam and L. Jiang, 2005. Estimation of the net radiation using MODIS (Moderate Resolution Imaging Spectroradiometer) data for clear sky days. *Remote Sens. Environ.* **97**, 52-67.

Cai X. L. and B. R. Sharma, 2010. Integrating remote sensing, census and weather data for an assessment of rice yield, water consumption and water productivity in the Indo-Gangetic river basin. *Agri. Water Manage.* **97**, 309-316.

Culf A. D., J. L. Esteves, A. O. Marques Filho and H. R. Rocha, 1996. Radiation, temperature and humidity over forest and pasture in Amazonia. In: *Amazonian deforestation and climate* (Gash, J. H. C., Nobre, C. A., Roberts, J. M. and Victoria, R. L. Eds.). New York, John Wiley & Sons, 175-191.

Di Pace F. T., B. B. Silva, V. P. R. Silva and S. T. A. Silva, 2008. Mapeamento do saldo de radiação com imagens Landsat 5 e modelo de elevação digital. *Revista Bras. Engenharia Agrícola e Ambiental* **12**, 385-392.

Galvão J. A. C. and G. Fisch, 2000. Balanço de radiação em área de pastagem na Amazônia. *Revista Brasileira de Agrometeorologia* **8**, 1-10.

Gao Y., D. Long and Z. Li, 2008. Estimation of daily actual evapotranspiration from remotely sensed data under complex terrain over the upper Chao river basin in North China. *Int. J. Remote Sens.* **29**, 3295-3315.

Malhi Y., J. T. Roberts, R. A. Betts, T. J. Killeen, W. Li and C. A. Nobre, 2008. Climate change, deforestation, and the fate of the Amazon. *Science* **319**, 169-172.

Melesse A. M, A. Frank, V. Nangia and J. Hanson, 2008. Analysis of energy fluxes and land surface parameters in a grassland ecosystem: a remote sensing perspective. *Int. J. Remote Sens.* **29**, 3325-3341.

Oguntoyinbo J. L., 1970. Reflection coefficient of natural crops and urban surfaces in Nigeria. *Q. J. Roy. Meteor. Soc.* **96**, 430-441.

Peres L. F. and C. C. DaCamara, 2004. Land surface temperature and emissivity estimation based on the two-temperature method: sensitivity analysis using simulated MSG/SEVIRI data. *Remote Sens. Environ.* **91**, 377-389.

Rimóczi-Paál A., 2005. Mapping of radiation balance components for region of Hungary using satellite information. *Phys. Chem. Earth* **30**, 151-158.

Roerink G. J., Z. Su and M. Menenti, 2000. S-SEBI: A Simple Remote Sensing Algorithm to Estimate the Surface Energy Balance. *Phys. Chem. Earth* **25**, 147-157.

Ryu Y., S. Kang, S. Moona and J. Kim, 2008. Evaluation of land surface radiation balance derived from moderate resolution imaging spectroradiometer (MODIS) over complex terrain and heterogeneous landscape on clear sky days. *Agr. Forest Meteorol.* **148**, 1538-1552.

Samani Z., A. S. Bawazir, M. Bleiweiss, R. Skaggs and V. D. Tran, 2007. Estimating daily net Radiation over Vegetation Canopy through Remote Sensing and Climatic Data. *J. Irrig. Drain. E.* **133**, 291-297.

Shuttleworth W. J., J. H. C. Gash, C. R. Lloyd, J. M. Roberts, A. O. Marques, G. Fisch, P. Silva, M. N. G. Ribeiro, L. C. B. Molion, L. D. A. Sá, C. A. Nobre, O. M. Cabral, S. R. Patel and J. C. Moraes, 1984. Observations of radiation exchange above and below Amazonian forest. *Q. J. Roy. Meteo. Soc.* **110**, 1163-1169.

Silva B. B., G. M. Lopes and P. V. Azevedo, 2005. Balanço de radiação em áreas irrigadas utilizando imagens Landsat 5 – TM. *Rev. Bras. Meteor.* **20**, 243-252.

von Randow C., A. O. Manzi, B. Kruijt, P. J. Oliveira, F. B. Zanchi, R. L. Silva, M. G. Hodnett, J. H. C. Gash, J. A. Elbers, M. J. Waterloo, F. L. Cardoso and P. Kabat, 2004. Comparative measurements and seasonal variations in energy and carbon exchange over forest and pasture in South West Amazonia. *Theor. Appl. Climatol.* **78**, 5-26.

Wang W. and S. Liang, 2009. Estimation of high-spatial resolution clear-sky longwave downward and net radiation over land surfaces from MODIS data. *Remote Sens. Environ.* **113**, 745-754.